

QuZO: Quantized Zeroth-Order Fine-Tuning for Large Language Models

Anonymous ACL submission

Abstract

Large Language Models (LLMs) are often quantized to lower precision to reduce the memory cost and latency in inference. However, quantization often degrades model performance, thus fine-tuning is required for various down-stream tasks. Traditional fine-tuning methods such as stochastic gradient descent and Adam optimization require back-propagation, which are error-prone in the low-precision settings. To overcome these limitations, we propose the Quantized Zeroth-Order (QuZO) framework, specifically designed for fine-tuning LLMs through low-precision (e.g., 4- or 8-bit) forward passes. Our method avoids the low-precision straight-through estimator, which requires backward computation, and instead utilizes optimized stochastic rounding to mitigate increased bias. QuZO simplifies the training process, while achieving results comparable to first-order methods in FP8 and superior accuracy in INT8 and INT4 training. Experiments demonstrate that QuZO achieves competitive performance on classification, multi-choice, and generation tasks under low-bit training, including zero-shot reasoning tasks. Notably, QuZO incurs minimal overhead and reduces memory consumption by $2.94\times$ – $5.47\times$ compared to quantized first-order methods during LLaMA-7B fine-tuning.

1 Introduction

Large Language Models (LLMs) have achieved state-of-the-art performance in natural language processing, impacting various science and engineering fields. However, deploying and fine-tuning LLMs consumes significant hardware resources because of their huge model size. To address this issue, extensive research has focused on LLM quantization (Brown et al., 2020a; Yuan et al., 2024). Notable approaches include post-training quantization (Yao et al., 2022; Wu et al., 2023), quantization-aware training (Bhalgat et al., 2020;

Liu et al., 2023c; Nagel et al., 2021), and fully quantized training (Choukroun et al., 2019; Xi et al., 2023; Markidis et al., 2018). Post-training quantization can effectively reduce the latency and memory costs of inference, but often leads to a significant accuracy drop in low-precision formats, although various techniques (Shao et al., 2023; Xiao et al., 2023; Lin et al., 2023; Liu et al., 2023c) can partially mitigate this issue. Quantization-aware training (Liu et al., 2023a) offers better accuracy, but is more expensive due to the use of high-precision computational graphs. Truly quantized training methods employ low-precision gradients, activation, and weights to reduce hardware costs (Wang et al., 2018b; Banner et al., 2018; Micikevicius et al., 2017). However, implementing truly quantized training requires advanced hardware and software support for both forward and backpropagation (BP). Meanwhile, the straight-through estimator (Yin et al., 2019), which is commonly used for quantized gradient estimations, often causes unstable and inaccurate results in low-bit training.

In practice, LLM users may afford only a low-cost LLM inference engine (e.g., an edge FPGA or embedded system) with limited precision (e.g., INT8 or INT4). This paper asks the following question: *Can we leverage inference-only quantized hardware to fine-tune low-bit LLMs while achieving good performance?* This seems challenging because (1) inference-only hardware lacks sufficient memory bandwidth and storage to retain intermediate activations required for backpropagation, and (2) the Straight-Through Estimator (STE) introduces increasing gradient approximation errors in lower-bit formats (Malinovskii et al., 2024).

The recent MeZO (Malladi et al., 2024) enables memory-efficient zeroth-order (ZO) fine-tuning for LLMs, but suffers from an avoidable performance drop compared to first-order (FO) methods due to the bias and variance of ZO gradient estimation. In this paper, we show that a *quantized zeroth-order*

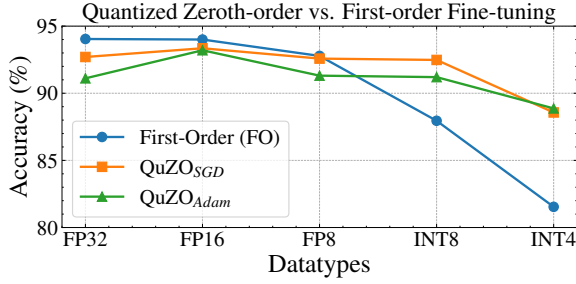


Figure 1: The proposed QuZO provides higher fine-tuning accuracy than first-order (FO) methods in ultra-low precision on the RoBERTa-Large model.

optimizer (QuZO) can achieve better accuracy than its first-order counterparts in a low-precision setting. Fig. 1 shows that both the QuZO and FO methods experience accuracy drops as the quantization precision decreases, which is expected. However, QuZO consistently outperforms FO methods when the quantization precision is INT8 or below. Unlike traditional FO quantized training that depends on the STE (Yin et al., 2019)-based BP method, our QuZO optimizer is more resistant to quantization error. Our contributions are summarized below.

- We identify the challenge of naive quantized ZO training, and propose a stochastic quantized perturbation method with theoretical soundness to reduce bias in quantized ZO gradient estimation.
- We introduce the implementation of QuZO as a plugin that integrates seamlessly with a quantized LLM inference engine, enabling accurate fine-tuning of low-bit LMs without backpropagation.
- We provide detailed numerical analysis about the proposed gradient estimator and the QuZO training framework. We show the benefit of our quantized ZO gradient estimator and the better training behavior of QuZO in low-bit LLM fine-tuning (especially INT4-format training).
- We apply QuZO to fine-tune 4/8-bit LLMs using both full-model fine-tuning and Low-Rank Adaptation (LoRA). QuZO achieves much better accuracy than quantized first-order training while reducing the memory cost by $1.4 \times -2.94 \times$.

2 Related Work

Zeroth-order method. Zeroth-order (ZO) optimization methods estimate gradients using only forward passes, thereby avoiding the need for backpropagation and significantly reducing memory consumption compared to first-order (FO) methods. MeZO (Malladi et al., 2024) employs a memory-efficient ZO stochastic gradient descent

(ZO-SGD) algorithm to fine-tune large language models (LLMs), leveraging parameter-efficient tuning methods such as LoRA (Yang et al., 2024b; Liu et al., 2022). However, MeZO does not consider low-bit model training or quantized perturbations, where naïve quantization often results in significant performance degradation. This limits its applicability in resource-constrained hardware scenarios that require both training and inference under low-precision constraints. Other ZO methods include ZO-SGD (Ghadimi and Lan, 2013) and ZO-Sign-SGD (Liu et al., 2018) using sign-based gradient estimation, the ZO-Adam (Chen et al., 2019) optimizer exploiting momentum information, and parameter-efficient methods like AdaZeta (Yang et al., 2024a). FP16 ZO training (Zhang et al., 2024) performs well but still faces memory bottlenecks. Recent ZO quantization introduces fixed-point 16-bit but fails at 8-bit (Feng et al., 2024). However, we overcome the challenges of lower-precision quantization and enable accurate fine-tuning of LLMs below 8-bit quantization.

Quantization of LLMs. Various quantization methods have been developed to reduce the memory and computing cost of LLMs. LLM.int8() (Dettmers et al., 2022) reduces the precision of model weights while keeping outliers in FP16. SmoothQuant (Xiao et al., 2023) introduces a fine-grained quantization method that supports INT8 operations exclusively. QLLM (Liu et al., 2023a) addresses the outlier problem via employing an adaptive channel reassembly technique. LLM-QAT (Liu et al., 2023c) employs Quantization-Aware Training (QAT) with a data-free strategy to achieve 4-bit quantization. Furthermore, the QuIP (Chee et al., 2023) and QLoRA (Dettmers et al., 2024) methods leverage a Hadamard Transform and a novel NF4 datatype, respectively, to accelerate training while preserving performance. While prior quantized training methods rely on backpropagation for gradient updates, our QuZO method eliminates the STE-based backpropagation and uses low-bit inference for truly quantized fine-tuning.

3 The QuZO Fine-Tuning Method

We start with a high-level introduction to our QuZO framework. Given a quantized LLM inference model, QuZO uses a low-bit ZO optimizer to update quantized model parameters directly during training. We assume that the forward pass

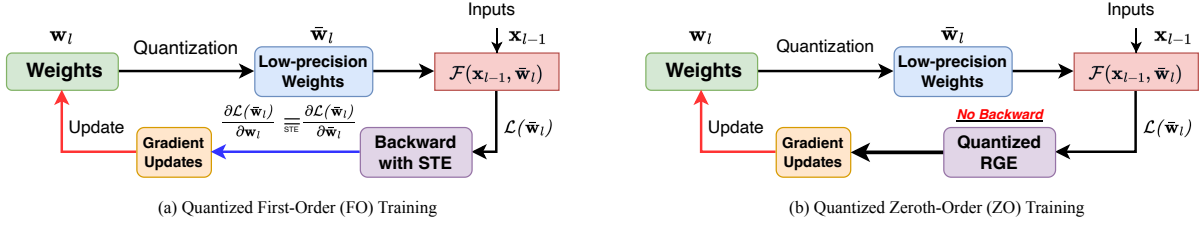


Figure 2: Computational graphs for quantized first-order (FO) and zeroth-order (ZO) training.

$\mathbf{x}_l = \mathcal{F}(\mathbf{x}_{l-1}, \bar{\mathbf{w}}_l)$ computes the output of the l -th layer using the quantized weight matrix $\bar{\mathbf{w}}_l$ and the previous-layer feature \mathbf{x}_{l-1} , as shown in Fig. 2 (b). With just a few forward passes, our QuZO framework uses quantized RGE (see Section 3.2) to estimate ZO gradients, eliminating the need for BP in model updates. This approach fundamentally differs from existing quantized training methods shown in Fig. 2 (a), which uses STE in the BP to approximate quantized gradient $\frac{\partial \mathcal{L}(\bar{\mathbf{w}})}{\partial \bar{\mathbf{w}}_l}$. Our method avoids the straight-through estimator (STE) (Yin et al., 2019) used in truly quantized FO training, enabling high-accuracy training on a low-precision hardware platform.

In the following, we first show the challenges of ZO-SGD in the quantized setting, and then propose a solution to address this fundamental challenge.

3.1 Challenges of Quantized ZO Training

Standard ZO-SGD uses a randomized gradient estimator (RGE) (Nesterov and Spokoiny, 2017; Ghadimi and Lan, 2013) to approximate a full-precision gradient. Specifically, given full-precision model parameters $\mathbf{w} \in \mathbb{R}^d$, a loss function $\mathcal{L}(\mathbf{w}, \mathcal{B})$ and a minibatch of dataset \mathcal{B} , RGE computes the gradient as:

$$\begin{aligned} \nabla \hat{\mathcal{L}}(\mathbf{w}) &= \sum_{i=1}^n \frac{\mathcal{L}_{\mathcal{B}}(\mathbf{w} + \epsilon \mathbf{u}_i) - \mathcal{L}_{\mathcal{B}}(\mathbf{w} - \epsilon \mathbf{u}_i)}{2n\epsilon} \mathbf{u}_i \\ &\approx \frac{1}{n} \sum_{i=1}^n \mathbf{u}_i \mathbf{u}_i^T \nabla \mathcal{L}_{\mathcal{B}}(\mathbf{w}), \end{aligned} \quad (1)$$

where ϵ is a scaling factor, $\{\mathbf{u}_i\}_{i=1}^n$ are i.i.d. samples drawn from certain distributions with a unit variance (e.g., a standard Gaussian distribution). While $\nabla \hat{\mathcal{L}}(\mathbf{w})$ differs from the true gradient $\nabla \mathcal{L}_{\mathcal{B}}(\mathbf{w})$, its expectation serves as a good gradient estimator because

$$\begin{aligned} \mathbb{E} [\nabla \hat{\mathcal{L}}(\mathbf{w})] &\approx \frac{1}{n} \sum_{i=1}^n \mathbb{E} (\mathbf{u}_i \mathbf{u}_i^T) \nabla \mathcal{L}_{\mathcal{B}}(\mathbf{w}) \\ &= \nabla \mathcal{L}_{\mathcal{B}}(\mathbf{w}). \end{aligned} \quad (2)$$

This statistical property ensures the asymptotical convergence of ZO-SGD. Assuming the quantized model parameters $\bar{\mathbf{w}}$ are available and only low-precision hardware is used for inference, the full-precision random perturbation \mathbf{u}_i cannot be directly applied to $\bar{\mathbf{w}}$ due to hardware limitations. To address this, \mathbf{u}_i is replaced with its quantized counterpart $\hat{\mathbf{u}}_i = Q(\mathbf{u}_i)$, leading to a low-precision RGE:

$$\begin{aligned} \nabla \hat{\mathcal{L}}(\bar{\mathbf{w}}) &= \sum_{i=1}^n \frac{\mathcal{L}_{\mathcal{B}}(\bar{\mathbf{w}} + \epsilon \hat{\mathbf{u}}_i) - \mathcal{L}_{\mathcal{B}}(\bar{\mathbf{w}} - \epsilon \hat{\mathbf{u}}_i)}{2n\epsilon} \hat{\mathbf{u}}_i \\ &\approx \frac{1}{n} \sum_{i=1}^n \hat{\mathbf{u}}_i \hat{\mathbf{u}}_i^T \nabla \mathcal{L}_{\mathcal{B}}(\bar{\mathbf{w}}). \end{aligned} \quad (3)$$

Taking the expectation on both sides, we have

$$\begin{aligned} \mathbb{E} [\nabla \hat{\mathcal{L}}(\bar{\mathbf{w}})] &\approx \frac{1}{n} \sum_{i=1}^n \mathbb{E} (\hat{\mathbf{u}}_i \hat{\mathbf{u}}_i^T) \nabla \mathcal{L}_{\mathcal{B}}(\bar{\mathbf{w}}) \\ &\neq \nabla \mathcal{L}_{\mathcal{B}}(\bar{\mathbf{w}}) \end{aligned} \quad (4)$$

Since the quantized perturbation $\hat{\mathbf{u}}_i = Q(\mathbf{u}_i)$ no longer maintains a unit variance, the above naive quantized RGE introduces bias during fine-tuning and may lead to divergence in training.

3.2 Proposed Quantized RGE

We propose a new quantized RGE scheme to address the challenge in the previous subsection.

Stochastic Quantization of \mathbf{u}_i . We first define a quantization operation of $Q(\mathbf{u}_i)$ based on stochastic rounding (Connolly et al., 2021):

$$\begin{aligned} Q(\mathbf{u}_i) &= \text{clamp}(SQ, L_{\min}, L_{\max}) + z_0, \\ SQ &= \left(\lfloor s_u \mathbf{u}_i \rfloor + \text{Ber}(s_u \mathbf{u}_i - \lfloor s_u \mathbf{u}_i \rfloor) \right) \end{aligned} \quad (5)$$

The stochastic quantization formula $Q(\mathbf{u}_i)$ converts the perturbation \mathbf{u}_i into a low-bit representation by scaling it with a factor s_u as $s_u \mathbf{u}_i$, performing a downward rounding operation $\lfloor s_u \mathbf{u}_i \rfloor$, and applying stochastic up-rounding using a Bernoulli random variable $\text{Ber}(s_u \mathbf{u}_i - \lfloor s_u \mathbf{u}_i \rfloor)$. The resulting quantized value is clamped to the representable

range $[L_{\min}, L_{\max}]$ and shifted by the zero point z_0 . This stochastic rounding ensures that

$$\mathbb{E}_Q [Q(\mathbf{u}_i)] = \mathbb{E} [\mathbf{u}_i]. \quad (6)$$

We can produce two different quantization results by using two random seeds in the stochastic rounding full-precision \mathbf{u}_i :

$$\begin{aligned} \mathbf{u}_{i,1} &= Q_1(\mathbf{u}_i) = Q(\mathbf{u}_i) \text{ with random seed } i_1; \\ \mathbf{u}_{i,2} &= Q_2(\mathbf{u}_i) = Q(\mathbf{u}_i) \text{ with random seed } i_2; \\ \mathbf{u}_{i,1} &\neq \mathbf{u}_{i,2}. \end{aligned} \quad (7)$$

The above stochastic quantizations ensure that (1) the expectation of the quantized perturbations $\mathbf{u}_{i,1}$ and $\mathbf{u}_{i,2}$ equals the original perturbation \mathbf{u}_i , (2) $\mathbf{u}_{i,1}$ and $\mathbf{u}_{i,2}$ are conditionally independent to each other. As a result, we have

$$\begin{aligned} \mathbb{E}_{Q_1}(\mathbf{u}_{i,1}) &= \mathbb{E}_{Q_2}(\mathbf{u}_{i,2}) = \mathbf{u}_i, \\ \mathbb{E}_{Q_1, Q_2}(\mathbf{u}_{i,1} \mathbf{u}_{i,2}^T) &= \mathbb{E}_{Q_1}(\mathbf{u}_{i,1}) \mathbb{E}_{Q_2}(\mathbf{u}_{i,2}^T) = \mathbf{u}_i \mathbf{u}_i^T. \end{aligned}$$

Our Quantized RGE. With the two conditionally independent quantized vectors $\mathbf{u}_{i,1}$ and $\mathbf{u}_{i,2}$ defined in Eq. (7), we propose the following quantized RGE:

$$\nabla \hat{\mathcal{L}}(\bar{\mathbf{w}}) = \sum_{i=1}^n \frac{\mathcal{L}_{\mathcal{B}}(\bar{\mathbf{w}} + \epsilon \mathbf{u}_{i,1}) - \mathcal{L}_{\mathcal{B}}(\bar{\mathbf{w}} - \epsilon \mathbf{u}_{i,1})}{2n\epsilon} \mathbf{u}_{i,2} \quad (8)$$

As $\epsilon \rightarrow 0$, the RGE result is

$$\nabla \hat{\mathcal{L}}(\bar{\mathbf{w}}) \approx \frac{1}{n} \sum_{i=1}^n \mathbf{u}_{i,1} \mathbf{u}_{i,2}^T \nabla \mathcal{L}_{\mathcal{B}}(\bar{\mathbf{w}}). \quad (9)$$

The estimation results depend on three random vectors and functions: \mathbf{u}_i , Q_1 and Q_2 . Taking expectation values on both sides of Eq. (9), we have

$$\begin{aligned} \mathbb{E} [\nabla \hat{\mathcal{L}}(\bar{\mathbf{w}})] &\approx \frac{1}{n} \sum_{i=1}^n \mathbb{E}_{\mathbf{u}_i, Q_1, Q_2} [\mathbf{u}_{i,1} \mathbf{u}_{i,2}^T] \nabla \mathcal{L}_{\mathcal{B}}(\bar{\mathbf{w}}) \\ &= \frac{1}{n} \sum_{i=1}^n \mathbb{E}_{\mathbf{u}_i} [\mathbb{E}_{Q_1, Q_2} [\mathbf{u}_{i,1} \mathbf{u}_{i,2}^T]] \nabla \mathcal{L}_{\mathcal{B}}(\bar{\mathbf{w}}) \\ &= \frac{1}{n} \sum_{i=1}^n \mathbb{E} (\mathbf{u}_i \mathbf{u}_i^T) \nabla \mathcal{L}_{\mathcal{B}}(\bar{\mathbf{w}}) \\ &= \nabla \mathcal{L}_{\mathcal{B}}(\bar{\mathbf{w}}). \end{aligned} \quad (10)$$

The expectation value of our quantized RGE remains a reliable estimator of the true gradient, which is similar to the full-precision RGE. This indicates that our proposed RGE will ensure asymptotical convergence as in a full-precision ZO method. This theoretical property ensures excellent training performance even in low-precision settings (e.g. INT8 and INT4).

3.3 Implementation of QuZO

Now we present the details of the implementation of the QuZO framework.

Quantized Model Updates. Recall that in full-precision ZO-SGD, the gradient is computed in (1), and the model parameters are updated as

$$\mathbf{w}_{t+1} = \mathbf{w}_t - \eta_t \cdot \nabla \hat{\mathcal{L}}(\mathbf{w}_t) \quad (11)$$

where \mathbf{w}_t represents the model parameters at iteration t , η_t is the learning rate and $\nabla \hat{\mathcal{L}}(\mathbf{w}_t)$ denotes the estimated gradient of the loss function. Since $\mathbf{w}_t \approx s_w \bar{\mathbf{w}}_t$, and s_w is a scaling factor used in the quantization $\bar{\mathbf{w}}_t = Q(\mathbf{w}_t/s_w)$, with $Q[\cdot]$ representing the stochastic quantization applied to the parameters. This approximation suggests:

$$\mathbf{w}_{t+1} \approx s_w [\bar{\mathbf{w}}_t - \eta_t \cdot \nabla \hat{\mathcal{L}}(\bar{\mathbf{w}}_t)] \quad (12)$$

To achieve a *truly quantized* training process suitable for low-precision hardware, the model parameters are updated as:

$$\bar{\mathbf{w}}_{t+1} = \bar{\mathbf{w}}_t - Q [\eta_t \cdot \nabla \hat{\mathcal{L}}(\bar{\mathbf{w}}_t)]. \quad (13)$$

To refine the update process, multiple steps can be used. For each query i , we compute

$$\mu_i = \frac{\mathcal{L}_{\mathcal{B}}(\bar{\mathbf{w}} + \epsilon \mathbf{u}_{i,1}) - \mathcal{L}_{\mathcal{B}}(\bar{\mathbf{w}} - \epsilon \mathbf{u}_{i,1})}{2\epsilon}. \quad (14)$$

Then the quantized model $\bar{\mathbf{W}}$ is updated as

$$\bar{\mathbf{w}}_{t+1} = \bar{\mathbf{w}}_t - \sum_{i=1}^n Q \left(\frac{\eta_t \mu_i}{n} \mathbf{u}_{i,2} \right). \quad (15)$$

Here $\mathbf{u}_{i,2}$ is a second quantized version of \mathbf{u}_i as explained in Eq. (7). Stochastic rounding $Q[\cdot]$ ensures that no additional bias will be introduced when we update the LLM parameters directly at low precision.

Algorithm Flow. The pseudo codes of QuZO are summarized in Algorithm 1. For each query i , two forward passes are performed to determine the sensitivity (μ_i) of the loss function with respect to a quantized perturbation direction $\mathbf{u}_{i,1}$ (lines 5-11). The resulting low-precision gradient associated with each inquiry is obtained by quantizing a scaled version of $\mathbf{u}_{i,2}$, where the sensitivity (μ_i), the learning rate η_t , and the sample size n are taken into account. This low-precision ZO gradient allows us to directly update the quantized LLM model parameters with low-precision hardware.

Algorithm 1 QuZO: Quantized Zeroth-Order Training

Require: LLM model parameters $\mathbf{w} \in \mathbb{R}^d$, learning rate η_t , T is the step, perturbation scaling factor ϵ and dataset \mathcal{B} .

```

1: Initial Pre-trained Model to Quantized Model or directly load a quantized model.
2:  $\bar{\mathbf{w}} = Q(\mathbf{w})$  ◁ Optionally, quantize the model if starting with a full-precision model
3: for  $t$  in  $T$  do
4:   for  $i$  in  $n$  do
5:      $\mathbf{u}_{i,1} \leftarrow Q_1(\mathbf{u}_i), \mathbf{u}_i \sim \mathcal{N}(0, \mathbb{I}_d)$  ◁ Quantize the perturbation  $\mathbf{u}_i$  with a random seed  $i_1$ 
6:      $\mathbf{u}_{i,2} \leftarrow Q_2(\mathbf{u}_i)$  ◁ Quantize the perturbation  $\mathbf{u}_i$  with a random seed  $i_2$ 
7:      $\bar{\mathbf{w}}_t \leftarrow \bar{\mathbf{w}}_t + \epsilon \cdot \mathbf{u}_{i,1}$  ◁ Low-bit stochastic perturbation updates  $\bar{\mathbf{w}}_t$  using positive scaling
8:      $\mathcal{L}_1^i \leftarrow \mathcal{F}(\bar{\mathbf{w}}_t, \mathcal{B})$  ◁ First zeroth-order forward pass
9:      $\bar{\mathbf{w}}_t \leftarrow \bar{\mathbf{w}}_t - 2\epsilon \cdot \mathbf{u}_{i,1}$  ◁ Low-bit stochastic perturbation updates  $\bar{\mathbf{w}}_t$  using negative scaling
10:     $\mathcal{L}_2^i \leftarrow \mathcal{F}(\bar{\mathbf{w}}_t, \mathcal{B})$  ◁ Second zeroth-order forward pass
11:     $\mu_i \leftarrow (\mathcal{L}_1^i - \mathcal{L}_2^i) / (2\epsilon)$  ◁ Sensitivity w.r.t. the quantized perturbation
12:     $\bar{\mathbf{w}}_t \leftarrow \bar{\mathbf{w}}_t + \epsilon \cdot \mathbf{u}_{i,1}$  ◁ Recover  $\bar{\mathbf{w}}_t$  to its original state
13:     $\bar{\mathbf{w}}_{t+1} \leftarrow \bar{\mathbf{w}}_t - Q(\frac{\eta_t \mu_i}{n} \mathbf{u}_{i,2})$  ◁ Quantized LLM model update
14:   end for
15: end for
16: return  $\bar{\mathbf{w}}$  ◁ Return a quantized model

```

QuZO for LoRA. We can extend the QuZO framework by incorporating low-rank adaptation to allow low-precision parameter-efficient fine-tuning. Our approach uses the model quantization strategies of QLoRA (Dettmers et al., 2024) and LLM.int8() (Dettmers et al., 2022) without modifying the quantized model. QuZO significantly reduces memory overhead by eliminating the storage of FO optimizer states and updating only the low-rank trainable matrices $\mathbf{A} \in \mathbb{R}^{d \times r}$ and $\mathbf{B} \in \mathbb{R}^{r \times d}$ using forward passes. In QuZO fine-tuning, the model parameters are quantized and frozen at low precision (e.g. 4 or 8 bits), and we update solely on the low-rank matrices \mathbf{A} and \mathbf{B} . The trainable low-rank matrices are quantized (denoted as $Q[\mathbf{A}]$ and $Q[\mathbf{B}]$) in order to match the precision of the LLM. By doing so QuZO training can significantly further reduce the memory cost compared to traditional LoRA for 4/8-bit LLM fine-tuning.

3.4 QuZO Analysis

In this subsection, we analyze the quality of gradient estimation in QuZO and its impact to training.

QuZO Gradient Quality. We use a simple encoder-block transformer to analyze the asymptotic behavior of two quantized ZO gradient estimators. Q-RGE1 refers to the quantized estimate in Eq. (3), and Q-RGE2 denotes our proposed estimation in Eq. (8). Although we need only a few inquiries to compute actual ZO gradients, the statistical behavior of a gradient (rather than the value of the individual gradient) decides the training performance. To verify statistical asymptotic behavior, we set $n = 1000$ to perform a Monte Carlo computation to get empirical mean values of Q-RGE1 and Q-RGE2, and then compare them with a full-

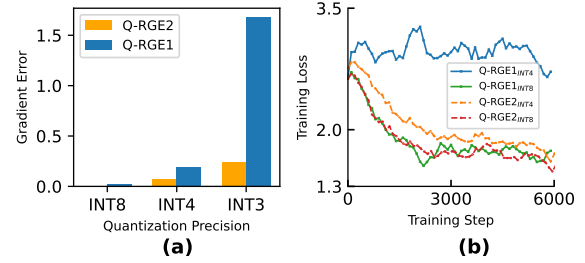


Figure 3: (a) Errors of quantized gradient estimation Q-RGE1 in Eq. (3) and our proposed Q-RGE2 in Eq. (8). (b) Training loss of low-precision ZO optimizer with these two quantized gradient estimators, respectively.

precision ZO gradient via the ℓ_2 error. As shown in Fig. 3 (a), the expected values of both quantized estimators have larger errors as the precision reduces from INT8 to INT3. However, our method (Q-RGE2) is much more resilient to quantization errors and has a more accurate expected value, since our quantized ZO gradient estimator can avoid the additional bias caused by quantization.

Training Behavior. Figure 3 (b) further shows the training behavior of quantized ZO optimization using these two gradient estimators when fine-tuning the OPT-1.3B model. Experiments are performed on the DROP dataset under 8-bit and 4-bit settings. We observe that our QuZO with Q-RGE2 shows slightly better convergence compared to quantized training using Q-RGE1 in the 8-bit setting. In 4-bit training, our method demonstrates a stable and significantly better training behavior: it achieves a loss similar to 8-bit training, while INT 4 Q-RGE1 causes convergence failures. The above analysis clearly demonstrates the better numerical performance of our QuZO in low-bit LLM fine-tuning.

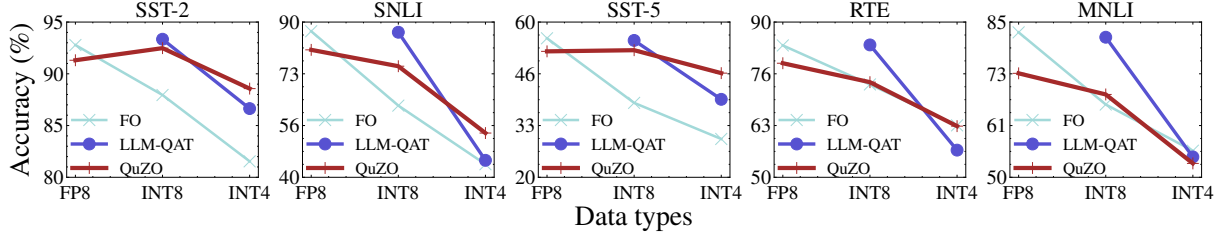


Figure 4: Experimental findings on RoBERTa-large (350M parameters) with prompts reveal that QuZO, leveraging full-parameter tuning, starts to surpass FO and LLM-QAT as precision reduces to INT8 or below.

Table 1: Results of low-bit LLM LoRA Fine-Tuning with quantized gradient updates.

Model	Methods	Gradient	MultiRC	ReCoRD	SQuAD	DROP
8bit LLaMa3-8B	FO	INT8	51.20	83.80	76.40	58.40
	MeZO	FP32	60.60	83.50	65.64	31.20
	QuZO	INT8	61.20	83.60	83.60	52.29
8bit Mistral-7B	FO	INT8	82.60	80.10	84.03	44.52
	MeZO	FP32	81.70	78.60	63.41	26.19
	QuZO	INT8	85.50	79.00	87.08	49.69
4bit LLaMa3-8B	FO	INT4	41.50	83.50	77.00	25.48
	MeZO	FP32	61.60	83.30	64.72	30.87
	QuZO	INT4	64.70	83.70	80.76	44.15
4bit Mistral-7B	FO	INT4	49.80	78.80	80.12	31.05
	MeZO	FP32	48.80	74.50	56.97	23.92
	QuZO	INT4	50.00	82.60	84.27	45.13

4 Experiments

In this section, we evaluate the proposed QuZO method on several language models (LMs) with 4-8 bit precision. QuZO demonstrates performance comparable to or better than standard first-order (FO) truly quantized training across various model sizes and tasks, with significantly lower memory usage. We also explore fine-tuning quantized models by combining QLoRA (Dettmers et al., 2024) with QuZO. For hardware costs, QuZO employs a forward-only framework with hardware requirements similar to post-training quantization. In Section 4.3, we compare the memory consumption between truly quantized FO training and QuZO. Furthermore, we employ both medium-size models (e.g. RoBERTa-Large (Liu et al., 2019)) and large decoder-based LMs, including OPT 1.3B (Zhang et al., 2022a) and LLaMa-2 7B (Touvron et al., 2023) LLaMa-3 8B and Mistral-v0.3-7B (Chaplot, 2023) in few-shot settings. Specifically, we evaluated PIQA (Bisk et al., 2020), ARC (Clark et al., 2018), HellaSwag (HS) (Zellers et al., 2019), and WinoGrande (WG) (Sakaguchi et al., 2021) with lm eval framework. All experiments were carried out on NVIDIA A100-40GB GPUs. The details of the experimental setup are in Appendix A.

4.1 Low-Bit LLM Fine-Tuning

Parameter-efficient fine-tuning methods like QLoRA (Dettmers et al., 2024) reduce memory usage with 4-bit precision compared to standard training but still rely on AdamW (Loshchilov, 2017), which requires backpropagation. QuZO improves inference efficiency and memory savings, achieving a $5.47\times$ reduction in maximum memory cost compared to QLoRA in fine-tuning the 4-bit OPT-1.3B model (details in Appendix C).

Our QuZO framework applies the LoRA (rank set as 8), allowing fine-tuning with far fewer trainable parameters than full-model tuning, significantly reducing memory consumption, and accelerating convergence. Table 1 highlights the performance of QuZO with low-bit perturbation and gradient configurations for different tasks and models. For the LLaMa3-8B model, QuZO utilizes INT8 RGE gradients with INT4 perturbations. Despite the introduction of low-bit gradients, QuZO achieves competitive or superior performance compared to full-precision MeZO with LoRA in most tasks and demonstrates strong robustness in 4-bit fine-tuning, while truly quantized FO shows poor accuracy in 4-bit training. For the Mistral-7B-v0.3 model, QuZO delivers the best performance on 3 out of 4 tasks, improving over FO by 3.05 on

Table 2: Zero-shot accuracy (%) on five commonsense reasoning tasks. Note : *WaAb* quantization, which refer to *a*-bit weight quantization and *b*-bit activation quantization.

Model	Quantization	Method	PIQA	ARC-e	ARC-c	HS	WG	Avg.
LLaMA-3 8B	FP16	Baseline	79.05	80.10	50.40	60.20	72.80	68.6
	W8A8	SmoothQuant	79.50	79.70	49.00	60.00	73.20	68.30
	W4A16	RTN	76.6	70.10	45.00	56.80	71.00	63.90
	W4A16	AWQ	79.10	79.70	49.30	59.10	74.00	68.20
	W4A16	QuIP	78.20	78.20	47.40	58.60	73.20	67.10
	W4A8	QServe	79.21	79.20	49.61	59.31	73.02	68.07
	W8A8	QuZO	78.74	80.03	50.06	59.34	74.03	68.43
	W4A16	QuZO	79.86	79.13	49.59	59.13	74.26	68.39

Table 3: QuZO demonstrates superior performance in full-parameter fine-tuning of LLaMa-2 7B.

LLaMa-2 7B Model		Classification			Multiple-Choice		Generation	
Data Precision	Method	RTE	WSC	MultiRC	COPA	ReCoRD	SQuAD	DROP
FP	FO	63.73	63.46	65.10	86.00	81.00	90.71	51.38
W16A32	MeZO	54.60	58.80	62.60	82.70	70.80	72.50	46.80
FP	FO	63.90	49.00	58.00	79.00	72.50	72.68	23.46
W8A8	QuZO	55.59	65.38	57.10	80.00	76.80	76.38	30.17
INT W8A8	FO	52.34	61.53	50.60	62.00	74.83	70.13	20.06
	SmoothQuant	66.78	59.51	61.50	72.02	79.10	73.07	29.94
	LLM.int8()	62.56	57.75	55.61	80.02	80.61	76.34	20.15
INT/FP W4A8	QuZO	61.01	63.46	60.00	81.00	79.00	77.71	30.11
	FO	47.29	60.57	51.90	62.04	73.21	30.01	10.06
	MinMax	59.91	41.28	53.21	82.51	80.97	50.07	24.71
	LLM-FP4	66.82	61.38	58.81	82.90	81.25	51.07	24.99
	QuZO	64.57	62.28	60.60	80.01	78.20	68.12	25.10

SQuAD and 2.9 on MultiRC. In the more challenging 4-bit setting, QuZO demonstrates notable robustness, with all perturbation precisions matching the gradient precision as shown in the Table 1. On Mistral-7B, QuZO again consistently outperforms both FO and MeZO, especially on SQuAD and DROP. This result shows that the low-bit stochastic perturbation of QuZO maintains comparable inference cost while mitigating quantization errors.

LLM Zero-Shot Reasoning. We evaluate QuZO on five widely-used commonsense reasoning benchmarks under the zero-shot setting using the LLaMA-3 8B model fine-tuned with our method. To ensure a fair comparison with recent quantization works (e.g., QServe (Lin et al., 2024), AWQ (Lin et al., 2023)) in Table 2, we adopt 4-bit and 8-bit precision. QuZO consistently outperforms other methods, achieving up to a 4.49% gain in average accuracy. Compared to the FP16 baseline, QuZO incurs only a marginal drop of 0.17% (W8A8) and 0.21% (W4A16), demonstrating its effectiveness under low-bit quantization settings.

4.2 Full-Parameter Quantized Fine Tuning

We summarize our experiments on full-parameter fine-tuning for medium- and large-scale models.

These results demonstrate that QuZO provides a practical approach for accurate fine-tuning of quantized LLMs directly on low-precision hardware, maintaining. For medium-scale models like RoBERTa-Large, QuZO surpasses truly quantized FO fine-tuning in most tasks in the 4-bit precision. For large-scale models such as LLaMA-2, QuZO achieves performance comparable to or better than truly quantized FO fine-tuning, particularly under ultra-low bit configurations. These findings highlight the ability of QuZO to enable low-cost hardware training without compromising performance.

Performance on the RoBERTa-Large model.

We evaluate the performance of various methods in the SST-2, SNLI, SST-5, RTE, and MNLI datasets and on the RoBERTa-Large model. The results in Fig. 4 leads to the following observations:

- As expected, all training methods experience accuracy decline as quantization precision decreases. This occurs because the model expressive power declines and the optimization becomes more challenging in lower precision.
- The performance of fully quantized FO fine-tuning drops most significantly due to the increasing errors in the straight-through estimators as precision decreases.

- QAT partially mitigates the accuracy drop of fully quantized FO training but still relies on backpropagation and full-precision updates, making it memory-intensive and less suited for low-precision hardware.
- In contrast, the performance of QuZO is **most resilient to the decreased precision**, and it works the best in a very low-precision (e.g., INT4). This is because (1) QuZO can bypass the error-prone straight-through estimator that is used in fully quantized FO training, and (2) the quantized RGE in Eqn.(8) can eliminate the bias caused by quantized perturbations.

Performance of QuZO on LLaMA Models. We further apply QuZO to fine-tune the LLaMa-2 model, evaluating it on SuperGLUE (Wang et al., 2019) and generation tasks. Table 3 shows that QuZO outperforms its truly quantized FO counterparts on all multichoice and generation tasks under FP W8A8 quantization (i.e. FP8 for both weights and activations). Under the INT W8A8 quantization, QuZO outperforms SmoothQuant, LLM.int8(), and truly quantized FO methods in 4 out of 7 tasks. For 4-bit quantized FO training, uniform quantization yields the worst accuracy, but advanced methods such as LLM-FP4 improve performance. LLM-FP4 (Liu et al., 2023b) and its baseline MinMax use FP W4A8 quantization and achieve a slight improvement in accuracy, particularly for multichoice tasks. QuZO demonstrates strong performance under W4A8 quantization, achieving the best results in 4 out of 7 tasks. In contrast, SmoothQuant, LLM.int8() and LLM-FP4 improve accuracy through efficient quantization but remain memory-intensive due to their reliance on first-order optimizers for fine-tuning.

4.3 Memory Efficiency

We further compare the empirical memory costs of full fine-tuning the LLaMA-2 7B model in Table 4. Specifically, in the MultiRC task, QuZO (8-bit) reduces memory usage by $1.43\times$ compared to their truly quantized FO counterparts. Similarly, in the SQuAD task, QuZO (4-bit) achieves a $2.89\times$ reduction relative to FO-SGD at the same precision. We follow Table 13 (see Appendix C) from (Zhang et al., 2024) to provide a theoretical analysis of different optimizers. Furthermore, QuZO reduces $2 - 5.47\times$ memory consumption

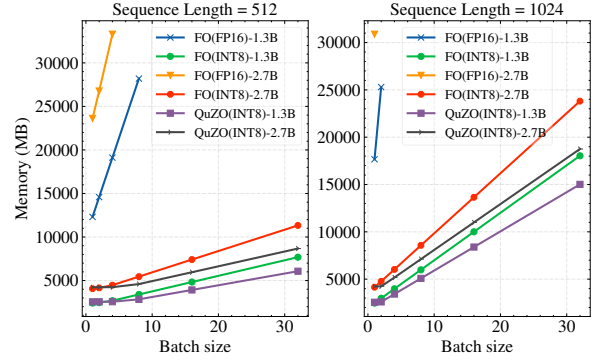


Figure 5: Peak memory usage of FP16 and INT8 training on the OPT 1.3B/2.7B model with sequence lengths of 512 (left) and 1024 (right).

Table 4: Total memory consumption (GB) for different optimizers on LLaMa-2 7B.

Method	MultiRC (GB)	SQuAD (GB)
FO-SGD (8-bit)	11.66	21.29
FO-SGD (4-bit)	6.28	10.73
QuZO (8-bit)	8.15	7.24
QuZO (4-bit)	4.52	3.71

compared to fully quantized FO methods in Table 14. A detailed memory efficiency analysis is included in Appendix C, where our QuZO demonstrates significant memory savings compared to truly quantized FO fine-tuning at the low precision.

To verify hardware efficiency, we profile the memory usage of our QuZO method with INT8 CUDA kernels, comparing it to the peak memory consumption of INT8 and FP16 tensor-core GEMM implementations in full parameter tuning. In practice, QuZO achieves up to a $7.8\times$ memory reduction with an INT8 model compared to the first-order FP16 training, as shown in Fig 5.

5 Conclusion

This work has proposed a Quantized Zeroth-Order (QuZO) method for truly quantized training of LLMs without using back propagation. We have identified the challenge of quantized ZO training, and proposed a new quantized ZO gradient to mitigate the bias in low-precision settings. QuZO eliminates the need for first-order optimizers such as Adam or SGD, as it relies on gradient-free updates derived from forward passes. The superior performance of QuZO in low-bit (e.g., INT8 and INT4) training has been shown by a variety of fine-tuning experiments on the LLaMA2/3 and Mistral-7B models. Our QuZO method is intrinsically hardware efficient for fine-tuning LLMs on low-bit resource-constrained hardware.

Limitations

The presented QuZO method can significantly impact practical LLM deployment. We have not yet implemented the real quantized training framework using low-precision kernels during training, as this requires much engineering effort. For instance, adding a minimal hardware block to an LLM inference accelerator can enable resource-efficient fine-tuning, making on-device learning of LLMs accessible and affordable for many downstream users. Additionally, QuZO can greatly reduce the latency and energy cost of fine-tuning due to its capability to directly use an ultra low-bit LLM inference accelerator. This will enable the deployment of LLMs in many resource-constrained scenarios, such as autonomous systems and robots.

References

- Ron Banner, Itay Hubara, Elad Hoffer, and Daniel Soudry. 2018. Scalable methods for 8-bit training of neural networks. *Advances in neural information processing systems*, 31.
- Yash Bhalgat, Jinwon Lee, Markus Nagel, Tijmen Blankevoort, and Nojun Kwak. 2020. Lsq+: Improving low-bit quantization through learnable offsets and better initialization. In *Proceedings of the IEEE/CVF conference on computer vision and pattern recognition workshops*, pages 696–697.
- Yonatan Bisk, Rowan Zellers, Jianfeng Gao, Yejin Choi, et al. 2020. Piqa: Reasoning about physical commonsense in natural language. In *Proceedings of the AAAI conference on artificial intelligence*, volume 34, pages 7432–7439.
- Samuel R Bowman, Gabor Angeli, Christopher Potts, and Christopher D Manning. 2015. A large annotated corpus for learning natural language inference. *arXiv preprint arXiv:1508.05326*.
- Tom Brown, Benjamin Mann, Nick Ryder, Melanie Subbiah, Jared D Kaplan, Prafulla Dhariwal, Arvind Neelakantan, Pranav Shyam, Girish Sastry, Amanda Askell, et al. 2020a. Language models are few-shot learners. *Advances in neural information processing systems*, 33:1877–1901.
- Tom Brown, Benjamin Mann, Nick Ryder, Melanie Subbiah, Jared D Kaplan, Prafulla Dhariwal, Arvind Neelakantan, Pranav Shyam, Girish Sastry, Amanda Askell, et al. 2020b. Language models are few-shot learners. *Advances in neural information processing systems*, 33:1877–1901.
- Devendra Singh Chaplot. 2023. Albert q. jiang, alexandre sablayrolles, arthur mensch, chris bamford, devendra singh chaplot, diego de las casas, florian bressand, gianna lengyel, guillaume lamplé, lucile

- saulnier, l  lio renard lavaud, marie-anne lachaux, pierre stock, teven le scao, thibaut lavril, thomas wang, timoth  e lacroix, william el sayed. *arXiv preprint arXiv:2310.06825*.
- Jerry Chee, Yaohui Cai, Volodymyr Kuleshov, and Christopher M De Sa. 2023. Quip: 2-bit quantization of large language models with guarantees. *Advances in Neural Information Processing Systems*, 36:4396–4429.
- Xiangyi Chen, Sijia Liu, Kaidi Xu, Xingguo Li, Xue Lin, Mingyi Hong, and David Cox. 2019. Zo-adamm: Zeroth-order adaptive momentum method for black-box optimization. *Advances in neural information processing systems*, 32.
- Yoni Choukroun, Eli Kravchik, Fan Yang, and Pavel Kisilev. 2019. Low-bit quantization of neural networks for efficient inference. In *2019 IEEE/CVF International Conference on Computer Vision Workshop (ICCVW)*, pages 3009–3018. IEEE.
- Peter Clark, Isaac Cowhey, Oren Etzioni, Tushar Khot, Ashish Sabharwal, Carissa Schoenick, and Oyvind Tafjord. 2018. Think you have solved question answering? try arc, the ai2 reasoning challenge. *arXiv preprint arXiv:1803.05457*.
- Michael P Connolly, Nicholas J Higham, and Theo Mary. 2021. Stochastic rounding and its probabilistic backward error analysis. *SIAM Journal on Scientific Computing*, 43(1):A566–A585.
- Tim Dettmers, Mike Lewis, Younes Belkada, and Luke Zettlemoyer. 2022. Gpt3. int8 (): 8-bit matrix multiplication for transformers at scale. *Advances in Neural Information Processing Systems*, 35:30318–30332.
- Tim Dettmers, Artidoro Pagnoni, Ari Holtzman, and Luke Zettlemoyer. 2024. Qlora: Efficient finetuning of quantized llms. *Advances in Neural Information Processing Systems*, 36.
- Dheeru Dua, Yizhong Wang, Pradeep Dasigi, Gabriel Stanovsky, Sameer Singh, and Matt Gardner. 2019. Drop: A reading comprehension benchmark requiring discrete reasoning over paragraphs. *arXiv preprint arXiv:1903.00161*.
- Chen Feng, Shaojie Zhuo, Xiaopeng Zhang, Ramchalam Kinattinkara Ramakrishnan, Zhaocong Yuan, and Andrew Zou Li. 2024. Stepping forward on the last mile. *arXiv preprint arXiv:2411.04036*.
- Elias Frantar, Saleh Ashkboos, Torsten Hoefer, and Dan Alistarh. 2022. Gptq: Accurate post-training quantization for generative pre-trained transformers. *arXiv preprint arXiv:2210.17323*.
- Natalia Frumkin, Dibakar Gope, and Diana Marculescu. 2023. Jumping through local minima: Quantization in the loss landscape of vision transformers. In *Proceedings of the IEEE/CVF International Conference on Computer Vision*, pages 16978–16988.

663	Tianyu Gao, Adam Fisch, and Danqi Chen. 2021.	Xiao Liu, Kaixuan Ji, Yicheng Fu, Weng Tam, Zhengx-	719
664	Making pre-trained language models better few-shot	iao Du, Zhilin Yang, and Jie Tang. 2022. P-tuning:	720
665	learners. In <i>Proceedings of the 59th Annual Meet-</i>	Prompt tuning can be comparable to fine-tuning	721
666	<i>ing of the Association for Computational Linguistics</i>	across scales and tasks. In <i>Proceedings of the 60th</i>	722
667	<i>and the 11th International Joint Conference on Natu-</i>	<i>Annual Meeting of the Association for Computational</i>	723
668	<i>ral Language Processing (Volume 1: Long Papers)</i> ,	<i>Linguistics (Volume 2: Short Papers)</i> , pages 61–68.	724
669	pages 3816–3830.		
670	Saeed Ghadimi and Guanghui Lan. 2013. Stochastic	Yinhan Liu, Myle Ott, Naman Goyal, Jingfei Du, Man-	725
671	first-and zeroth-order methods for nonconvex stochas-	dar Joshi, Danqi Chen, Omer Levy, Mike Lewis,	726
672	tic programming. <i>SIAM journal on optimization</i> ,	Luke Zettlemoyer, and Veselin Stoyanov. 2019.	727
673	23(4):2341–2368.	Roberta: A robustly optimized bert pretraining ap-	728
674	Eduard Hovy, Laurie Gerber, Ulf Hermjakob, Chin-	proach. <i>arXiv preprint arXiv:1907.11692</i> .	729
675	Yew Lin, and Deepak Ravichandran. 2001. Toward		
676	semantics-based answer pinpointing. In <i>Proceedings</i>	Yong Liu, Zirui Zhu, Chaoyu Gong, Minhao Cheng,	730
677	<i>of the first international conference on Human lan-</i>	Cho-Jui Hsieh, and Yang You. 2024. Sparse	731
678	<i>guage technology research</i> .	mezo: Less parameters for better performance	732
679	Sangil Jung, Changyong Son, Seohyung Lee, Jinwoo	in zeroth-order llm fine-tuning. <i>arXiv preprint</i>	733
680	Son, Jae-Joon Han, Youngjun Kwak, Sung Ju Hwang,	<i>arXiv:2402.15751</i> .	734
681	and Changkyu Choi. 2019. Learning to quantize deep		
682	networks by optimizing quantization intervals with	Zechun Liu, Barlas Oguz, Changsheng Zhao, Ernie	735
683	task loss. In <i>Proceedings of the IEEE/CVF confer-</i>	Chang, Pierre Stock, Yashar Mehdad, Yangyang	736
684	<i>ence on computer vision and pattern recognition</i> ,	Shi, Raghuraman Krishnamoorthi, and Vikas Chan-	737
685	pages 4350–4359.	dra. 2023c. Llm-qat: Data-free quantization aware	738
686	Sehoon Kim, Amir Gholami, Zhewei Yao, Michael W	training for large language models. <i>arXiv preprint</i>	739
687	Mahoney, and Kurt Keutzer. 2021. I-bert: Integer-	<i>arXiv:2305.17888</i> .	740
688	only bert quantization. In <i>International conference</i>		
689	<i>on machine learning</i> , pages 5506–5518. PMLR.	I Loshchilov. 2017. Decoupled weight decay regulariza-	741
690	Jangwhan Lee, Minsoo Kim, Seungcheol Baek,	tion. <i>arXiv preprint arXiv:1711.05101</i> .	742
691	Seok Joong Hwang, Wonyong Sung, and Jungwook		
692	Choi. 2023. Enhancing computation efficiency in	Ilya Loshchilov and Frank Hutter. 2018. Decoupled	743
693	large language models through weight and activation	weight decay regularization. In <i>International Confer-</i>	744
694	quantization. <i>arXiv preprint arXiv:2311.05161</i> .	<i>ence on Learning Representations</i> .	745
695	Ji Lin, Jiaming Tang, Haotian Tang, Shang Yang,	Vladimir Malinovskii, Denis Mazur, Ivan Ilin, Denis	746
696	Xingyu Dang, and Song Han. 2023. Awq: Activation-	Kuznetsov, Konstantin Burlachenko, Kai Yi, Dan	747
697	aware weight quantization for llm compression and	Alistarh, and Peter Richtarik. 2024. Pv-tuning: Be-	748
698	acceleration. <i>arXiv preprint arXiv:2306.00978</i> .	yond straight-through estimation for extreme llm	749
699	Yujun Lin, Haotian Tang, Shang Yang, Zhekai Zhang,	compression. <i>arXiv preprint arXiv:2405.14852</i> .	750
700	Guangxuan Xiao, Chuang Gan, and Song Han.		
701	2024. Qserve: W4a8kv4 quantization and system	Sadhika Malladi, Tianyu Gao, Eshaan Nichani, Alex	751
702	co-design for efficient llm serving. <i>arXiv preprint</i>	Damian, Jason D Lee, Danqi Chen, and Sanjeev	752
703	<i>arXiv:2405.04532</i> .	Arora. 2024. Fine-tuning language models with just	753
704	Jing Liu, Ruihao Gong, Xiuying Wei, Zhiwei Dong,	forward passes. <i>Advances in Neural Information</i>	754
705	Jianfei Cai, and Bohan Zhuang. 2023a. Qllm: Accu-	<i>Processing Systems</i> , 36.	755
706	rate and efficient low-bitwidth quantization for large		
707	language models. <i>arXiv preprint arXiv:2310.08041</i> .	Stefano Markidis, Steven Wei Der Chien, Erwin Laure,	756
708	Shih-yang Liu, Zechun Liu, Xijie Huang, Pingcheng	Ivy Bo Peng, and Jeffrey S Vetter. 2018. Nvidia ten-	757
709	Dong, and Kwang-Ting Cheng. 2023b. LLM-FP4:	sor core programmability, performance & precision.	758
710	4-bit floating-point quantized transformers . In <i>Pro-</i>	In <i>2018 IEEE international parallel and distributed</i>	759
711	<i>ceedings of the 2023 Conference on Empirical Meth-</i>	<i>processing symposium workshops (IPDPSW)</i> , pages	760
712	<i>ods in Natural Language Processing</i> , pages 592–605,	522–531. IEEE.	761
713	Singapore. Association for Computational Linguis-		
714	tics.	Paulius Micikevicius, Sharan Narang, Jonah Alben, Gre-	762
715	Sijia Liu, Pin-Yu Chen, Xiangyi Chen, and Mingyi	gory Diamos, Erich Elsen, David Garcia, Boris Gins-	763
716	Hong. 2018. signsgd via zeroth-order oracle. In	burg, Michael Houston, Oleksii Kuchaiev, Ganesh	764
717	<i>International Conference on Learning Representa-</i>	Venkatesh, et al. 2017. Mixed precision training.	765
718	<i>tions</i> .	<i>arXiv preprint arXiv:1710.03740</i> .	766
		Markus Nagel, Marios Fournarakis, Rana Ali Amjad,	767
		Yelysei Bondarenko, Mart Van Baalen, and Tijmen	768
		Blankevoort. 2021. A white paper on neural network	769
		quantization. <i>arXiv preprint arXiv:2106.08295</i> .	770
		Yurii Nesterov and Vladimir Spokoiny. 2017. Ran-	771
		dom gradient-free minimization of convex func-	772
		tions. <i>Foundations of Computational Mathematics</i> ,	773
		17(2):527–566.	774

775	Pranav Rajpurkar, Robin Jia, and Percy Liang. 2018.	Xiaoxia Wu, Zhewei Yao, and Yuxiong He. 2023.	828
776	Know what you don't know: Unanswerable questions	Zeroquant-fp: A leap forward in llms post-training	829
777	for squad. <i>arXiv preprint arXiv:1806.03822</i> .	w4a8 quantization using floating-point formats.	830
		<i>arXiv preprint arXiv:2307.09782</i> .	831
778	Pranav Rajpurkar, Jian Zhang, Konstantin Lopyrev, and	Haocheng Xi, Changhao Li, Jianfei Chen, and Jun Zhu.	832
779	Percy Liang. 2016. Squad: 100,000+ questions	2023. Training transformers with 4-bit integers. <i>Ad-</i>	833
780	for machine comprehension of text. <i>arXiv preprint</i>	<i>advances in Neural Information Processing Systems</i> ,	834
781	<i>arXiv:1606.05250</i> .	36:49146–49168.	835
782	Keisuke Sakaguchi, Ronan Le Bras, Chandra Bhagavat-	Guangxuan Xiao, Ji Lin, Mickael Seznec, Hao Wu,	836
783	ula, and Yejin Choi. 2021. Winogrande: An adver-	Julien Demouth, and Song Han. 2023. Smoothquant:	837
784	sarial winograd schema challenge at scale. <i>Communi-</i>	Accurate and efficient post-training quantization for	838
785	<i>ications of the ACM</i> , 64(9):99–106.	large language models. In <i>International Conference</i>	839
		<i>on Machine Learning</i> , pages 38087–38099. PMLR.	840
786	Wenqi Shao, Mengzhao Chen, Zhaoyang Zhang, Peng	Yifan Yang, Kai Zhen, Ershad Banijamali, Athanasios	841
787	Xu, Lirui Zhao, Zhiqian Li, Kaipeng Zhang, Peng	Mouchtaris, and Zheng Zhang. 2024a. Adazeta:	842
788	Gao, Yu Qiao, and Ping Luo. 2023. Omniquant:	Adaptive zeroth-order tensor-train adaption for	843
789	Omnidirectionally calibrated quantization for large	memory-efficient large language models fine-tuning.	844
790	language models. <i>arXiv preprint arXiv:2308.13137</i> .	In <i>Proceedings of the 2024 Conference on Empiri-</i>	845
		<i>cal Methods in Natural Language Processing</i> , pages	846
791	Richard Socher, Alex Perelygin, Jean Wu, Jason	977–995.	847
792	Chuang, Christopher D Manning, Andrew Y Ng, and	Yifan Yang, Jiajun Zhou, Ngai Wong, and Zheng Zhang.	848
793	Christopher Potts. 2013. Recursive deep models for	2024b. Loretta: Low-rank economic tensor-train	849
794	semantic compositionality over a sentiment treebank.	adaptation for ultra-low-parameter fine-tuning of	850
795	In <i>Proceedings of the 2013 conference on empiri-</i>	large language models. In <i>Proceedings of the 2024</i>	851
796	<i>cal methods in natural language processing</i> , pages	<i>Conference of the North American Chapter of the</i>	852
797	1631–1642.	<i>Association for Computational Linguistics: Human</i>	853
798	Tianxiang Sun, Zhengfu He, Hong Qian, Yunhua Zhou,	<i>Language Technologies (Volume 1: Long Papers)</i> ,	854
799	Xuanjing Huang, and Xipeng Qiu. 2022. Bbtv2: To-	pages 3161–3176.	855
800	wards a gradient-free future with large language mod-		
801	els. <i>arXiv preprint arXiv:2205.11200</i> .	Zhewei Yao, Reza Yazdani Aminabadi, Minjia Zhang,	856
		Xiaoxia Wu, Conglong Li, and Yuxiong He. 2022.	857
802	Hugo Touvron, Thibaut Lavril, Gautier Izacard, Xavier	Zeroquant: Efficient and affordable post-training	858
803	Martinet, Marie-Anne Lachaux, Timothée Lacroix,	quantization for large-scale transformers. <i>Advances</i>	859
804	Baptiste Rozière, Naman Goyal, Eric Hambro,	<i>in Neural Information Processing Systems</i> , 35:27168–	860
805	Faisal Azhar, et al. 2023. Llama: Open and effi-	27183.	861
806	cient foundation language models. <i>arXiv preprint</i>	Penghang Yin, Jiancheng Lyu, Shuai Zhang, Stanley	862
807	<i>arXiv:2302.13971</i> .	Osher, Yingyong Qi, and Jack Xin. 2019. Un-	863
		derstanding straight-through estimator in training	864
808	Alex Wang, Yada Pruksachatkun, Nikita Nangia, Aman-	activation quantized neural nets. <i>arXiv preprint</i>	865
809	preet Singh, Julian Michael, Felix Hill, Omer Levy,	<i>arXiv:1903.05662</i> .	866
810	and Samuel Bowman. 2019. Superglue: A stick-	Zhihang Yuan, Yuzhang Shang, Yang Zhou, Zhen Dong,	867
811	ier benchmark for general-purpose language under-	Chenhao Xue, Bingzhe Wu, Zhikai Li, Qingyi Gu,	868
812	standing systems. <i>Advances in neural information</i>	Yong Jae Lee, Yan Yan, et al. 2024. Llm inference	869
813	<i>processing systems</i> , 32.	unveiled: Survey and roofline model insights. <i>arXiv</i>	870
		<i>preprint arXiv:2402.16363</i> .	871
814	Alex Wang, Amanpreet Singh, Julian Michael, Felix	Rowan Zellers, Ari Holtzman, Yonatan Bisk, Ali	872
815	Hill, Omer Levy, and Samuel R Bowman. 2018a.	Farhadi, and Yejin Choi. 2019. Hellaswag: Can a	873
816	Glue: A multi-task benchmark and analysis platform	machine really finish your sentence? <i>arXiv preprint</i>	874
817	for natural language understanding. <i>arXiv preprint</i>	<i>arXiv:1905.07830</i> .	875
818	<i>arXiv:1804.07461</i> .		
819	Naigang Wang, Jungwook Choi, Daniel Brand, Chia-Yu	Susan Zhang, Stephen Roller, Naman Goyal, Mikel	876
820	Chen, and Kailash Gopalakrishnan. 2018b. Train-	Artetxe, Moya Chen, Shuohui Chen, Christopher De-	877
821	ing deep neural networks with 8-bit floating point	wan, Mona Diab, Xian Li, Xi Victoria Lin, et al.	878
822	numbers. <i>Advances in neural information processing</i>	2022a. Opt: Open pre-trained transformer language	879
823	<i>systems</i> , 31.	models. <i>arXiv preprint arXiv:2205.01068</i> .	880
824	Adina Williams, Nikita Nangia, and Samuel R Bow-	Yan Zhang, Yi Zhou, Kaiyi Ji, and Michael M Za-	881
825	man. 2017. A broad-coverage challenge corpus for	vlanos. 2022b. A new one-point residual-feedback	882
826	sentence understanding through inference. <i>arXiv</i>	oracle for black-box learning and control. <i>Automat-</i>	883
827	<i>preprint arXiv:1704.05426</i> .	<i>ica</i> , 136:110006.	884

- 885 Yihua Zhang, Pingzhi Li, Junyuan Hong, Jiayang Li,
886 Yimeng Zhang, Wenqing Zheng, Pin-Yu Chen, Ja-
887 son D Lee, Wotao Yin, Mingyi Hong, et al. 2024.
888 Revisiting zeroth-order optimization for memory-
889 efficient llm fine-tuning: a benchmark. In *Proceed-*
890 *ings of the 41st International Conference on Machine*
891 *Learning*, pages 59173–59190.
- 892 Yanli Zhao, Andrew Gu, Rohan Varma, Liang Luo,
893 Chien-Chin Huang, Min Xu, Less Wright, Hamid
894 Shojanazeri, Myle Ott, Sam Shleifer, et al. 2023. Py-
895 torch fsdp: experiences on scaling fully sharded data
896 parallel. *arXiv preprint arXiv:2304.11277*.
- 897 Jiajun Zhou, Jiajun Wu, Yizhao Gao, Yuhao Ding, Chao-
898 fan Tao, Boyu Li, Fengbin Tu, Kwang-Ting Cheng,
899 Hayden Kwok-Hay So, and Ngai Wong. 2023. Dybit:
900 Dynamic bit-precision numbers for efficient quan-
901 tized neural network inference. *IEEE Transactions*
902 *on Computer-Aided Design of Integrated Circuits*
903 *and Systems*.

Appendix

A Experiments Setup

We first conduct experiments with RoBERTa-large on sentiment classification and natural language classification tasks. We follow prior works (Malladi et al., 2024) in low data resource settings which can be sampling k examples per class for $k = 16$ or 512. QuZO is running for 100k steps and the first order fine-tuning for 5 epochs. We also conducted experiments on a smaller set of tasks (Wang et al., 2018a) that includes entailment, span sentiment analysis, and topic classification. These tasks include perceptual analysis (SST-2 and SST-5 (Socher et al., 2013)), Question Classification (TREC (Hovy et al., 2001)), and natural language reasoning (MNLI, SNLI, and RTE (Bowman et al., 2015; Williams et al., 2017; Rajpurkar et al., 2018)). The metrics we used for the GLUE benchmark are summarized in Table 5.

Table 5: Metrics that we use to evaluate GLUE Benchmark for BERT-based Model.

Task Name	Metric
SST-2	Accuracy
SST-5	Accuracy
MNLI	Matched Acc.
SNLI	Accuracy
TREC	Accuracy
RTE	Accuracy

Subsequently, we selected several SuperGLUE tasks (Wang et al., 2019), encompassing classification (CB, BoolQ, WSC) and multiple-choice (COPA and ReCoRD), alongside two additional question-answering tasks (SQuAD (Rajpurkar et al., 2016) and DROP (Dua et al., 2019)). To intensify the challenge, we operated under the few-shot setting, randomly sampling 1,000 examples for training, 500 for validation, and 1,000 for testing. We followed the prompt settings outlined in Appendix D of the MeZO (Malladi et al., 2024) to adapt classification tasks into language model tasks. The evaluation metrics used are summarized in Table 6. All experiments were conducted using the AdamW optimizer (Loshchilov and Hutter, 2018).

A.1 Hyperparameters

As observed in some LLM fine-tuning literature, zeroth-order (ZO) optimization typically shows consistent performance improvement with training

Table 6: Metrics that we use to evaluate SuperGLUE and generations tasks.

Task Name	Metric
CB	F1
BoolQ	Accuracy
WSC	F1
COPA	Accuracy
ReCoRD	F1
SQuAD	F1
DROP	F1

Table 7: The hyperparameter grids used for RoBERTa-Large experiments.

Experiment	Hyperparameters	Values
FO	Batch size	[8, 16]
	Learning rate	$1e-5, 1e-6$
LLM-QAT	Batch size	[8, 16]
	Learning rate	$5e-6$
QuZO	Batch size	[16, 64]
	Learning rate	$1e-6, 1e-7$
	ϵ	$1e-5$
	Weight Decay	0, 0.1

steps. However, the number of forward passes significantly affects computational costs. To optimize resource usage, we limit the training steps to 10k for the RoBERTa-Large model on the SST-2, SST-5, TREC, MNLI, and SNLI datasets. In Table 7, our method primarily use a batch size of 64 and experiment with different learning rates for RoBERTa-Large fine-tuning (Fig. 4). Since first-order (FO)-based methods use the Adam optimizer, both FO and LLM-QAT (Liu et al., 2023c) experiments utilize smaller batch sizes and larger learning rates compared to ZO tuning. We use the hyperparameters in Table 7 for the RoBERTa-Large model. Note that even though we run all experiments for 5 epochs, further learning steps may help to improve the performance of our proposed methods further.

Regarding the LLaMa-2 7B model, we use the hyperparameters in Table 8. We evaluate the model for around 10-12k training steps and directly use the last checkpoint for evaluation. All first-order (FO) quantization training experiments train for 5 epochs and all QuZO experiments use 12K steps.

Table 8: The hyperparameter grids used for LLaMA-2 experiments.

Experiment	Hyperparameters	Values
QLoRA	Batch size	[2, 4, 8, 16]
	Learning rate	$1e-5, 5e-6, 5e-7$
LLM.int8()	Batch size	[2, 4, 8, 16]
	Learning rate	$1e-5, 5e-6, 5e-7$
MeZO	Batch size	[8, 16]
	Learning rate	$1e-4, 5e-5, 5e-6$
QuZO	Batch size	[4, 8, 16]
	Learning rate	$1e-4, 5e-5, 5e-6$

Modeling and implementation The model and prompt-tuning process follows a structured approach tailored for RoBERTa-large, OPT, and LLaMa-2 models across various tasks. For RoBERTa, a masked language model (MLM) fine-tuning paradigm is used, where prompts incorporate [MASK] tokens that the model learns to predict, with specific label word mappings defining classification outputs. Tasks such as sentiment classification (SST-2, SST-5), topic classification (TREC), and natural language inference (MNLI, SNLI, RTE) utilize template-based prompts adapted from prior works (Gao et al., 2021).

For OPT and LLaMa-2, the tuning process follows GPT-3-style prompting (Brown et al., 2020b) and encompasses three task categories: classification, multiple-choice, and question answering (QA). Classification tasks rely on cross entropy loss for label prediction, while multiple-choice and QA tasks utilize teacher forcing to train on correct outputs. During inference, classification and multiple-choice predictions are determined using the average log-likelihood per token, whereas QA responses are generated through greedy decoding. Additionally, in-context learning with 32-shot examples is employed to maintain stable results.

For classification tasks, RoBERTa uses linear probing, while OPT and LLaMa employ LM head tuning to refine task-specific representations. This fine-tuning framework ensures consistent evaluation across datasets and models, leveraging structured prompts to enhance adaptability in both low-data and fully supervised settings.

Full Parameter Tuning Performance of QuZO on OPT Models We further evaluate our method on the OPT-1.3B model using quantization-aware training. The activation functions of OPT models are generally more sensitive to quantization errors

compared to the LLaMA model, posing some challenges for LLM quantization. In Table 9, our QuZO method outperforms quantization methods such as QLLM and SmoothQuant in 8 out of 11 tasks under the INT W8A8 quantization.

B Quantization Methods

In this section, we present our weight-activation quantization method. Since per-channel activation quantization is incompatible with efficient GEMM kernels, we employ per-tensor static activation quantization as our coarsest-grained quantization method and per-channel weight quantization as our finer-grained quantization scheme. For post-training quantization (PTQ) methods, we adopt the quantization configuration from SmoothQuant and evaluate their W8A8 quantization under our low data resource setting. Additionally, we reproduce LLM-FP4 (Liu et al., 2023b) using their open-source codebases and evaluate the same tasks within their frameworks, noting that it requires significant time for datatype searching. To ensure a fair comparison, we reduce the calibration size to 8.

B.1 Weight-only Quantization

Throughout this work, we focus initially on both weight and activation quantization. This approach can introduce significant quantization errors and lead to accuracy degradation. To address this, we further evaluate weight-only quantization on several tasks, as detailed in Table 10. Our findings indicate that weight-only quantization yields better performance compared to combined weight and activation quantization. There are some related work that only do weight quantization for LLMs (i.e GPTQ (Frantar et al., 2022)). But it converts the quantized weight to FP16 on the fly during inference and lead to speed up.

B.2 Hybrid Datatype Support

Mixed Datatypes Support. Assigning the same low-bit datatype to both weights and activations in QuZO can lead to accuracy degradation due to the limited precision of 4-bit integers compared to floating-point formats, with activation functions being particularly sensitive to quantization errors. While QLoRA introduced the NF4 datatype to mitigate this issue, our QuZO framework takes it a step further by assessing quantization errors (Jung et al., 2019) for hybrid formats at the same precision. This mixed-datatype fine-tuning in quantized

Table 9: Performance comparisons for weights and activations quantization on the OPT-1.3B model.

OPT-1.3B Model		Classification							Multiple-Choice		Generation	
Data Precision	Method	SST-2	RTE	CB	BoolQ	WSC	WIC	MultiRC	COPA	ReCoRD	SQuAD	DROP
INT W8A8	QLLM	82.45	55.59	66.07	63.00	63.46	52.35	56.81	71.01	59.90	61.49	15.80
	LLM.int8	53.66	53.79	41.07	46.32	42.31	58.46	45.72	75.00	70.22	67.14	10.33
	SmoothQuant	75.01	52.34	37.51	48.20	44.23	57.83	53.41	71.03	68.81	69.42	11.22
	QuZO(FT)	91.38	55.61	67.85	62.30	63.46	60.03	55.91	74.00	70.81	73.88	21.82

Table 10: Weight-only Quantization experiments conducted on LLaMa-2 7B model.

LLaMa-2 7B Model		Classification					Multiple-Choice		Generation	
Data Precision	Method	SST-2	RTE	CB	BoolQ	MultiRC	COPA	ReCoRD	SQuAD	DROP
INT-W4A32	QuZO(FT)	92.43	60.28	60.71	65.50	59.60	83.00	79.00	82.78	37.31
INT-W8A32	QuZO(FT)	92.77	62.81	71.42	64.00	60.70	83.00	81.00	80.93	40.25
FP-W8A32	QuZO(FT)	93.69	61.37	66.07	63.72	60.91	81.01	79.60	80.93	37.86

ZO training effectively preserves performance even under 4-bit quantization. Existing works (Liu et al., 2023c; Zhou et al., 2023) also incorporate this into their quantization strategy but require customized hardware to support the specific datatype. In our quantization algorithm, we use a set of quantization grids $\mathbf{b} = \{b_1, b_2, \dots, b_i\}$ and apply the quantization operation $Q_b(w)$ to map a full-precision scalar w to a quantized value as follows:

$$Q_b(w) = b_i, i = \operatorname{argmin} |w - b_i|.$$

This notation indicates the parameter w is quantized to the closest quantization grid point b_i . We denote the corresponding quantization error as $\mathbb{E}_b(w) = Q_b(w) - w$. We use the mean squared error (MSE) as the metric to calculate the quantization loss:

$$\text{MSE} = \mathbb{E}[(w - Q_b(w))^2] \quad (16)$$

where w are the FP32 value, and $p(w)$ stands for the probability density function. The neural network weights are a random variable $w \sim p_w(w)$. The quantization range is defined between b_{\min} and b_{\max} . Our framework selects the data type that minimizes the MSE for each layer and executes the searching algorithm only once before fine-tuning. Based on our data-type search algorithm, we found that INT quantization is more suitable for weight quantization, offering better hardware efficiency. On the other hand, FP quantization is primarily chosen for activation quantization to maintain good accuracy. This quantization selection offers a more accurate QuZO fine-tuning process.

Underflow severely impacts low-bit quantization in

LLMs (Lee et al., 2023), associated with rounding zero values that further degrade model performance. Therefore, we propose a hybrid datatype search in Section 4.2 during quantized zeroth-order training, using existing data formats, including integers and floating-points, which are widely used in hardware platforms. We evaluate the LLaMA-2 model using the hybrid datatype detailed in Table 11. Through coarse layer-wise datatype selection, QuZO can boost around 1 to 2% average performance across these 11 tasks in both W4A8 and W8A8 quantization.

B.3 Quantized Perturbation

We now explore the ZO gradient quantization, which can accelerate model training without compromising convergence. Using a fully quantized I-BERT (Kim et al., 2021) as an example, we assign low-bit perturbation to update the INT8 model, as shown in Table 12. The accuracy drop is less than 1%, but the memory reduction is around 4-16 \times for the random perturbation parameters. In the RoBERTa-Large model, we found that 2-bit perturbation performs better, indicating that quantized perturbation does not significantly affect training performance. This is a huge benefit for ZO training since the perturbations are generated and calculated four times for one training step. Current works only focus on sparse parameter perturbations (Liu et al., 2024) for reducing gradient estimation variance in RGE. It introduces the masks and applies them to weight perturbations per step. However, we now consider on hardware-efficient side and use low-precision weight perturbation to do ZO gradient estimation in LLM fine-tuning. We further analyze

Table 11: Compared to pure-INT or FP quantized zero-order training, our hybrid datatype (INT and FP) searching algorithm boosts accuracy by 1-2% for most tasks on the LLaMa-2 7B model.

LLaMa-2 7B Model			Classification							Multiple-Choice		Generation		Avg
Method	Datatype	Precision	SST-2	RTE	CB	BoolQ	WSC	WIC	MultiRC	COPA	ReCoRD	SQuAD	DROP	Performance
QuZO(Ours)	INT	W4A8	89.10	54.87	62.50	66.60	64.42	57.99	60.60	83.00	78.20	78.12	31.80	66.10
QuZO(Ours)	INT/FP	W4A8	90.59	59.92	63.71	68.40	64.50	59.70	59.30	80.00	78.60	79.89	33.55	67.10
QuZO(Ours)	INT	W8A8	93.00	61.01	64.18	80.00	63.46	52.82	60.01	81.00	79.00	77.71	31.11	67.58
QuZO(Ours)	INT/FP	W8A8	93.08	65.95	64.28	81.10	64.57	55.17	60.11	83.00	79.60	80.74	36.58	69.47

Table 12: Evaluate the impact of low-bit perturbation on QuZO training for SST-2 tasks using different models.

Model	Model Precision	Perturbation (#bit)	Performance
I-BERT	INT W8A8	8	92.77
I-BERT	INT W8A8	4	92.48
I-BERT	INT W8A8	2	91.89
RoBERTa-Large	INT W8A8	8	92.48
RoBERTa-Large	INT W8A8	4	91.51
RoBERTa-Large	INT W8A8	2	93.07
LLaMa-2 7B	INT W4A8	8	91.32

the memory costs of the perturbation parameters $\mathbf{u} \in \mathbb{R}^d$. At each step, QuZO reuses \mathbf{u} four times in Algorithm 1. We evaluated the quantized perturbation experiments on the RoBERTa-Large model, and it costs around 1.63 GB of memory to store each \mathbf{u} during one step. However, quantized perturbation would only cost 110 to 410 MB if we quantize it to 2-bit or 8-bit, respectively. Since these results are estimated based on the number of perturbations and storage datatype, a real hardware implementation is required to demonstrate the full advantage. We will address this in future work.

Handling outliers. The outliers mainly occur in the activations of transformers and can severely degrade quantization performance if not addressed efficiently (Liu et al., 2023c,a; Lin et al., 2023). To simplify the quantization process without introducing overhead, we propose an outlier detector that can distinguish outliers from normal values. Our outlier detector can automatically select the outlier threshold to determine a suitable ratio α (Outliers/All data), which is normally around 1%. We quantize the normal data using a pre-defined quantization datatype and quantize the outlier data using the same precision FP type. As a signed INT8 quantization example, we designate the binary code 10000000_2 as an outlier label to identify outlier values in the selected tensor array. Consequently, the valid data range becomes $[-127, 127]$, and we utilize an 8-bit floating-point scheme with adaptive biased bits to efficiently quantize these outlier values. It enables efficient quantization of LLMs across various hardware platforms such as

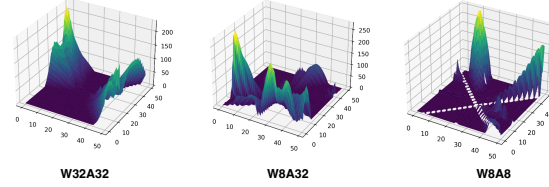


Figure 6: The loss landscape of the RoBERTa-large model under different quantization bits. The notations W and A mean the bits for weights and activation.

CPU and FPGAs using the QuZO method.

Loss Landscape. The effectiveness of ZO fine-tuning for LLMs arises from starting near the optimal loss region. Theoretical analysis in (Malladi et al., 2024) [Lemma 3] links ZO convergence to the low effective rank of Hessian matrix. In quantized training, the Lipschitz smoothness constant L significantly impacts performance (Frumkin et al., 2023). Fig. 6 (See Appendix B) demonstrates the stability of the smoothness of loss function across weight and activation quantization levels, underscoring the effectiveness in low-bit ZO training.

B.4 ZO Gradient Accumulation

Gradient accumulation is a technique for training models where data samples are divided into several batches and calculated sequentially. To fine-tune large models on a single GPU, especially for datasets like DROP that require small batch sizes, we implemented a zeroth-order accumulation method for performing weight updates. Initially, we calculate the gradient without updating the network parameters at each step, accumulating the projected gradient information. After reaching the predefined accumulation steps, the accumulated gradient is used to update the parameters. We also incorporate prevalent efficiency-enhancing tricks adopted in current zeroth-order optimizers, following the first-order approach to implement our zeroth-order method effectively. This approach allows efficient fine-tuning of large models on a single GPU, leveraging the advantages of gradient accumulation within a QuZO optimization framework.

Table 13: Comparison of peak memory consumption during full-model fine-tuning. Note: model storage (Weight Mem.) and dynamic allocations for gradients (Dynamic Mem.). $|w|$ and $|a|$ denote memory usage for model parameters and intermediate parameters, respectively, with l representing a specific layer.

Method	Weight Mem.	Dynamic Mem
Full Precision Optimizer		
FO-SGD	$ w $	$\sum_l \max \{ a , w \}$
MeZO	$ w $	$\max_l w $
Optimizer with Low Precision Model		
FO(8-bit)	$ w /4$	$\sum_l \max \{\frac{ a }{4}, \frac{ w }{4}\}$
FO(4-bit)	$ w /8$	$\sum_l \max \{\frac{ a }{8}, \frac{ w }{8}\}$
QuZO(8-bit)	$ w /4$	$\max_l \frac{ w }{4}$
QuZO(4-bit)	$ w /8$	$\max_l \frac{ w }{8}$

C Hardware Efficiency of QuZO

To demonstrate the hardware efficiency of QuZO, we employ the Cutlass INT8 Kernel to showcase memory efficiency. To fine-tune large models efficiently with limited GPUs, we assess the first-order (FO) method using Fully Sharded Data Parallelism (FSDP) (Zhao et al., 2023) for distributed training. Besides, We believe it can be further reduced if we fully apply the INT engine in each linear and non-linear layer. This could be our next step in the CUDA optimization. Finally, we provide the memory cost of our QuZO method using INT8 CUDA kernels and compare it with the peak memory usage of INT8 and FP16 tensor-core GEMM implementations on full parameter tuning. As the batch size increases from 1 to 32, the memory reduction reaches up to $7.8\times$ when running with an INT8 model compared to FP16 training in Fig. 5.

Table 14: Memory Consumption (GB) Across Models and Methods for Five Tasks. This table compares the memory requirements of different methods (e.g., LLM.int8, QuZO, and QLoRA) across various tasks using two models: OPT1.3B and LLaMa-2 7B. The QuZO method demonstrates significantly lower memory consumption across all models, while LLM.int8() encounters Out of Memory (OOM) issues in some cases.

Model	Methods	SST-2	MultiRC	ReCoRD	SQuAD	DROP
8-bit OPT 1.3B	LLM.int8()	9.01	23.97	6.76	22.09	31.29
	QuZO	3.43	12.61	4.82	7.50	16.42
4-bit OPT 1.3B	QLoRA	4.76	18.15	4.42	20.48	27.23
	QuZO	1.72	6.30	2.41	3.74	11.70
8-bit LLaMa-2 7B	LLM.int8()	31.47	OOM	19.06	OOM	OOM
	QuZO	9.94	25.11	13.04	16.69	31.66

Table 15: Runtime comparison (seconds per step) on OPT-30B model using DROP dataset. QuZO achieves strong per-step efficiency while operating on a single GPU.

Model Size	FO (FP32)	FO (4-bit)	MeZO (FP32)	QuZO (4-bit)
OPT-30B	45.61s (8 GPUs)	~22.80s (8 GPUs)	4.267s (2 GPUs)	~2.84s (1 GPU)

C.1 Memory Efficiency

Table 14 provides a comprehensive comparison of memory consumption (in GB) across various tasks when fine-tuning quantized models using QuZO with LoRA ($rank = 8$). The methods compared include QuZO, LLM.int8(), and QLoRA. Notably, QuZO employs 4-bit perturbations to fine-tune the models, achieving significant memory savings compared to LLM.int8 and QLoRA. For instance, in the OPT1.3B-int4 model, QuZO reduces memory usage by approximately $2.8\times$ on SST-2 (1.72 GB vs. 4.76 GB in QLoRA) and by $5.47\times$ on SQuAD (3.74 GB vs. 20.48 GB in QLoRA). Similarly, for the OPT1.3B-int8 model, QuZO achieves a memory reduction of $1.4\times$ on MultiRC (12.61 GB vs. 23.97 GB in INT8 FO fine tuning).

In the 8-bit LLaMa-2 7B model, while LLM.int8 encounters Out-of-Memory (OOM) errors on several tasks, QuZO successfully completes fine-tuning with substantial memory efficiency, using just 9.94 GB on SST-2 compared to 31.47 GB for LLM.int8—a reduction of $3.2\times$. These results highlight the ability of QuZO to fine-tune quantized models effectively with minimal memory overhead, leveraging 4-bit perturbations for substantial efficiency gains while maintaining compatibility with LoRA architectures. This positions QuZO as a practical choice for resource-constrained fine-tuning in large-scale NLP tasks.

C.2 Runtime Comparison on Large-Scale Models

To clarify the computational advantages of QuZO, we conducted runtime experiments on the OPT-30 B model using the DROP dataset. All models were tested on 40GB A100 GPUs. As shown in Table 15, QuZO achieves a significant speedup over both first-order (FO) and full-precision MeZO methods. For example, FO (FP32) requires 45.61 seconds per training step using 8 GPUs, while MeZO reduces this to 4.27 seconds on fewer resources. In contrast, QuZO (4-bit) further improves efficiency, taking only 2.84 seconds per step. This translates to approximately $1.5\times$ speedup over MeZO and $16\times$

speedup over FO. Although zeroth-order methods typically require more steps (e.g., MeZO may need up to $32\times$ more), the per-step efficiency and single-GPU execution result in fewer total GPU-hours. In particular, QuZO reduces GPU-hour consumption by roughly $2\times$ compared to FO (4-bit), and about $4\times$ compared to FO (full-precision), demonstrating its scalability and practical utility for large LLM training.

D Ablation Study of QuZO

These experiments evaluate key components of our method, including the number of perturbations (queries) per update and the sparsity of the stochastic perturbation vectors. We then compare the performance of Q-RGE1 and Q-RGE2 when fine-tuning the LLaMA-2 13B model under the same precision settings. Additionally, we compare different backpropagation-free (BP-free) training methods and extend our evaluation to larger-scale models such as LLaMA-2 70B. This provides a comprehensive assessment of various ZO variants.

D.1 Effect of Query Number

We investigate how the number of perturbation queries influences performance and convergence. Increasing the number of queries per step leads to more accurate gradient estimation, which improves fine-tuning effectiveness. Table 16 shows that increasing the number of queries from 1 to 10 results in a 3.6% improvement in DROP accuracy. From our experiments, using a larger number of queries accelerates training convergence but increases the time per step.

Table 16: Varying query number on DROP performance.

Model	Task	Query=1	Query=5	Query=10
LLaMa-13B (8-bit)	DROP	37.61	39.77	41.33

Table 17: Perturbation sparsity on downstream task performance.

Model	Sparsity	ReCoRD	SQuAD	DROP
QuZO (8-bit)	0%	82.20	80.29	37.61
QuZO (8-bit)	20%	82.60	80.52	34.65
QuZO (8-bit)	50%	82.50	81.21	40.51
QuZO (8-bit)	80%	83.00	80.10	25.99

D.2 Effect of Perturbation Sparsity

We also analyze the impact of perturbation sparsity, defined as the percentage of zero entries in the stochastic perturbation vector during training. Higher sparsity reduces the number of trainable parameters and speeds up training. Table 17 shows that QuZO maintains strong performance even with 50% sparsity, while higher sparsity (e.g., 80%) leads to some performance degradation, especially on the DROP dataset. Notably, increasing sparsity improves training speed by $1.2\times$ to $2\times$. These results confirm that QuZO is robust to both reduced query counts and perturbation sparsity, offering practical trade-offs between accuracy and training efficiency.

D.3 Comparison Between Q-RGE1 and Q-RGE2

We have explicitly evaluated Q-RGE1 in actual experiments and clearly demonstrate that our proposed Q-RGE2 (QuZO) significantly outperforms it in Fig 3. Specifically, we conducted training comparisons using the LLaMA-13B model on the ReCoRD, SQuAD, and DROP datasets under both 4-bit and 8-bit quantization settings.

As shown in Table 18, Q-RGE2 consistently yields substantial accuracy improvements—exceeding 10% in challenging tasks like SQuAD. These results highlight the performance benefits achieved by Q-RGE2, further validating its effectiveness and robustness in low-bit quantized training scenarios.

Table 18: Performance comparison between Q-RGE1 and Q-RGE2 (QuZO) on LLaMA-13B under 4-bit and 8-bit quantization.

Method	Model	ReCoRD	SQuAD	DROP
Q-RGE1	LLaMA-13B (8-bit)	81.80	64.23	24.88
Q-RGE2 (Ours)	LLaMA-13B (8-bit)	82.20	78.19	37.61
Q-RGE1	LLaMA-13B (4-bit)	81.60	63.02	25.15
Q-RGE2 (Ours)	LLaMA-13B (4-bit)	82.10	73.79	27.32

Table 19: Comparison with other gradient-free methods on 4-bit LLaMA2-7B model.

Method	Model (bits)	SST-2	SNLI	RTE
In-Context Learning	LLaMA-7B (4-bit)	85.01	49.65	51.21
One-Point Estimator	LLaMA-7B (4-bit)	89.96	53.56	48.24
QuZO (Ours)	LLaMA-7B (4-bit)	91.62	64.40	54.87

D.4 Gradient-Free Fine-Tuning Comparison

While few existing approaches have been directly applied to large-scale language model (LLM) fine-

Table 20: Performance Comparison of QuZO on the LLaMa-2 13B Model

Model (#Bit)	Methods	ReCoRD	SQuAD	DROP
LLaMa2-13B (8-Bit)	FO	81.70	63.23	25.90
	MeZO	82.10	63.71	25.20
	QuZO	82.20	78.19	37.61
LLaMa2-13B (4-Bit)	FO	82.00	62.27	25.31
	MeZO	82.30	62.62	25.33
	QuZO	82.10	73.79	27.32

Table 21: Results on LLaMA-70B using a single GPU vs. FO with 4 GPUs.

Method	Model	Computational Card (GB)	SQuAD	DROP
FO	LLaMA-70B (4-bit)	4x A100 (158GB)	76.78	51.84
QuZO	LLaMA-70B (4-bit)	1x A100 (37GB)	81.25	58.11

tuning, we compare QuZO with the One-Point Estimator (Zhang et al., 2022b), a relevant zeroth-order method. Although Black-Box Tuning (BBT) (Sun et al., 2022) adopts gradient-free optimization via evolutionary strategies, its scalability to high-dimensional full-model tuning in LLMs remains limited. As shown in Table 19, the One-Point Estimator achieves lower computational cost (about $2\times$ faster than QuZO) but suffers significant accuracy drops across all tasks. In contrast, QuZO demonstrates strong stability and superior performance, highlighting its robustness in low-bit, gradient-free fine-tuning scenarios.

D.5 Large-size LLMs

Table 20 presents the performance comparison of QuZO fine-tuning against other methods with LoRA, including First-Order (FO) and MeZO, on the LLaMa-2 13B model under 8-bit and 4-bit quantization. The evaluation is conducted on three datasets: ReCoRD, SQuAD, and DROP, which assess reading comprehension and reasoning ability. The results indicate that QuZO consistently outperforms MeZO and FO, particularly in SQuAD and DROP, demonstrating its ability to better retain performance in a quantized setting. In the 8-bit setting, QuZO achieves a significant improvement. In the 4-bit setting, the trend remains similar, highlighting the robustness of QuZO in handling more aggressive quantization.

Fine-Tuning 70B LMs. Specifically, we fine-tuned the LLaMA-70B (4-bit) model using QuZO and compared them against traditional first-order (FO) methods. Following a similar instruction-style prompting setup as in MeZO, we reformulate question answering and reasoning benchmarks using

fixed task-specific prompts. This design enables evaluation of QuZO within a practical instruction-tuning framework, without requiring backpropagation. The results show consistent improvements across standard QA datasets such as SQuAD, as well as reasoning tasks like DROP.